

# Lawrence Berkeley National Laboratory

## LBL Publications

### Title

Ultra-low blaze angle gratings for synchrotron and free electron laser applications.

### Permalink

<https://escholarship.org/uc/item/2fv4k0c8>

### Journal

Optics Express, 26(17)

### ISSN

1094-4087

### Authors

Voronov, DL

Gullikson, EM

Padmore, HA

### Publication Date

2018-08-20

### DOI

10.1364/oe.26.022011

Peer reviewed



# Ultra-low blaze angle gratings for synchrotron and free electron laser applications

D. L. VORONOV,\* E. M. GULLIKSON, AND H. A. PADMORE

Lawrence Berkeley National Laboratory, 1 Cyclotron Road, Berkeley, CA 94720, USA

\*[dlvoronov@lbl.gov](mailto:dlvoronov@lbl.gov)

**Abstract.** We have developed a method for the manufacture of x-ray diffraction gratings with arbitrarily small blaze angles. These gratings are made by a process in which a high blaze angle grating made by anisotropic etching of Si (111) is subjected to planarization and reactive ion etching. Differential etching of the planarization medium and silicon ensures reduction of the blaze angle. Repeated application of this process leads to gratings of increasing perfection with an arbitrarily small blaze angle. This opens the way to highly efficient low line density gratings, to damage resistant gratings for ultra-high power applications such as free electron lasers, and for extension of the use of gratings into the hard x-ray energy range for dispersive spectroscopy.

© 2018 Optical Society of America under the terms of the [OSA Open Access Publishing Agreement](#)

## 1. Introduction

X-ray diffraction gratings are widely used at synchrotron facilities around the world. Parameters of the gratings may vary in a wide range depending on a specific application. For example, high resolution spectroscopy requires high dispersion which can be achieved by use of high groove density gratings [1,2]. On the other hand, x-ray microscopy, ptychography, tomography, lithography etc., a high photon flux is the priority which can be achieved by low dispersion x-ray gratings due to their high diffraction efficiency and substantial bandwidth. Such gratings should have a low groove density and a very small blaze angle. For example, the monochromator of the Cosmic beamline at the Advanced Light Source designed for coherent scattering and microscopy experiments is equipped with 4 gratings of groove density of 100 and 300 lines/mm [3]. The optimal blaze angles of the gratings would be in the range of 0.17 - 0.35°. However, such gratings are extremely challenging to fabricate and lamellar gratings are used instead. Although lamellar gratings are available commercially they have lower diffraction efficiency which substantially reduces the throughput of the monochromator.

Similar blazed gratings are needed for Free Electron Laser (FEL) applications [4] since they offer much higher stability over lamellar gratings which suffer from laser ablation damage of their rectangular grooves [5]. The off-plane diffraction mount of lamellar gratings was suggested to avoid ablation and achieve high diffraction efficiency [6]. This however requires rather complicated monochromator design [7].

Only extremely grazing incidence optics can withstand the extreme high power of the laser and avoid surface damage owing to the spread of the power load over a large area. The grazing geometry leads to very low groove density and ultra-low blaze angles of the gratings [8,9]. The maximum photon energy that gratings are used at is limited by the grazing angle required for high reflectivity, leading to a requirement for very small blaze angles. Although gratings are traditionally used up to a photon energy of 2.5 keV, there is no reason why gratings cannot be used in the hard x-ray domain. Although Bragg crystals exist to cover this energy range, they have a very limited angular reflection range, leading to a very narrow diffracted energy width. While this is useful for high resolution spectroscopy, it is a problem for dispersive spectroscopy. For example, one of the main methods to understand chemical bonding is the technique of extended x-ray absorption fine structure (EXAFS), where the x-ray absorption signal is monitored from an elemental absorption edge. The required energy

range at the iron K edge might be from 7 to 8 keV. Although crystal-based dispersive spectrometers exist, they are angle selecting, i.e. one angle on the crystal corresponds to one energy. The great advantage of a grating spectrograph is that a very wide range of wavelengths can be dispersed and focused from any point on the grating. The necessary requirement though is for a very small blaze angle, typically around  $0.1^\circ$ , commensurate with the small grazing angles that have to be used.

Diamond ruling is currently the main method of making blazed gratings for x-rays. Since it is challenging to rule perfectly triangular grooves with blazed angles smaller than  $3\text{-}5^\circ$ , an additional process of reduction of the blaze angle is required. In this process, the blazed grooves ruled into a metal layer are transferred to the underlying Si substrate by an ion beam etching process [4,8,9]. Owing to the difference in the sputter yield of the metal and Si under bombardment by high energy ions of a noble gas, the transferred grating has a reduced groove depth and a lower blaze angle. Adding Oxygen to the sputter gas mixture increases the reduction factor due to the Si oxidation chemistry involved. The main drawback of this approach is the extremely low speed of the ruling process, causing a high cost of the gratings.

An alternative process for low blaze grating fabrication based on anisotropic wet etching of silicon by alkali solutions was demonstrated recently [10]. The method exploits a difference in etch rates of a Si surface with respect to the (111) planes of the Si single crystal. The tilt of the blazed facets is defined by the angular offset of the Si crystal surface with respect to the (111) planes. The method provides a perfect groove shape for high groove density gratings with blaze angles in the range of  $2\text{-}6^\circ$  [11,12]. However, making coarse gratings with blaze angles less than  $1^\circ$  is troublesome since the anisotropy of the etching reduces dramatically as the grating blank surface approaches to the (111) plane. Etching of shallow and coarse grooves can take a very long period of time, which usually is accompanied by etching instabilities, surface contaminations etc. leading to deterioration of the grating quality. Moreover, blazed facets of the etched gratings are slightly concave rather than perfectly plane. This is not an issue for high groove density and/or high blaze angle gratings since the grating efficiency is not affected considerably until the facet sag is substantially smaller than the groove depth. However, for extremely low blaze angle gratings the groove depth can be as small as a few tens of nanometers and the facet curvature may cause substantial efficiency loss [10].

To address the challenges mentioned above we developed a two-stage process for making high quality gratings with low groove density and ultra-small blaze angles. We fabricate a Si blazed grating with a relatively large blaze angle by use of anisotropic wet etching and then we reduce the blaze angle of the grating down to a required value. In this paper we report on development of a process for reduction of the blaze angle below  $0.2^\circ$ .

## 2. Fabrication process flow

The proposed reduction process is based on planarization and reactive ion etching (RIE) as illustrated in Fig. 1. A Si grating with a relatively large blaze angle [Fig. 1(a)] is coated with a sacrificial layer which provides planarization of the saw-tooth surface [Fig. 1(b)]. The following RIE provides etching both of the sacrificial layer and the silicon grating with the etch rates  $V_{SL}$  and  $V_{Si}$  respectively. The resulting shape of the grating grooves is defined by the ratio of etch rates of Si and the sacrificial layer. The groove height will be changed by a reduction factor  $R = 1/(1 - V_{Si}/V_{SL})$ . If the etch rate of the sacrificial layer is much higher than the etch rate of Si ( $V_{Si}/V_{SL} \ll 1$ ) the sacrificial layer will be etched off with no change in the groove shape of the Si grating ( $R = 1$ ). If the etch rates are the same ( $V_{Si}/V_{SL} = 1$ ) the top surface of the sacrificial layer will be transferred to the Si resulting in smoothing out the grating grooves ( $R = \infty$ ). An intermediate etch rate ratio ( $0 < V_{Si}/V_{SL} < 1$ ) is expected to result in reduction of the groove depth and the blazed angle of the Si grating as schematically shown in Figs. 1(c) and 1(d). Note, if  $V_{Si}/V_{SL} > 1$  the grooves profile will flip and the blaze angle can even increase as compared to the original saw-tooth grating.

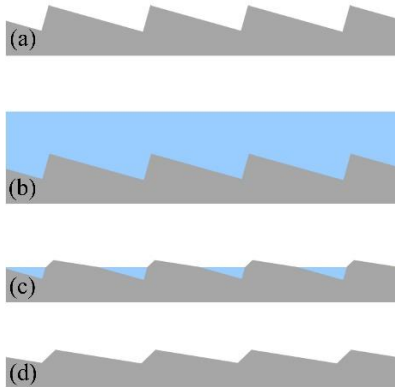


Fig. 1. Process flow for reduction of the blaze angle of an original saw-tooth grating: original Si grating with large blaze angle (a), planarization of the grating surface with a sacrificial layer (b), plasma etching of the sacrificial layer with an etch rate of  $V_{SL}/V_{Si} \approx 2$  (c), a final blazed grating with a reduced blaze angle (d).

To demonstrate feasibility of the approach we aimed for fabrication of a 100 lines/mm test grating with a blaze angle of  $0.17^\circ$ . The grating is a prototype of the most challenging blazed grating for the Cosmic monochromator.

### 3. Blaze angle reduction

A  $25 \times 25 \text{ mm}^2$  test grating with a period of  $10 \mu\text{m}$  was fabricated by use of KOH anisotropic wet etching of a (111) Si wafer, miscut by an angle of  $6^\circ$  towards the  $11\bar{2}$  direction. Dimensions of the test grating were large enough for the proof-of-principle experiment and the efficiency measurements (see Section 4). The details of the fabrication process were described elsewhere [10–12]. An AFM image of the etched grating finalized with an isotropic etching with a  $\text{SF}_6$  plasma is shown in Fig. 2(a). The grating has a blaze angle of  $5.7^\circ$  and groove depth of about  $1 \mu\text{m}$ .

We used an AR3 antireflective coating from Rohm and Haas Electronic Materials [13] as a sacrificial layer. Preliminary tests showed that the etch rate of the AR3 in a fluorine-based plasma is approximately twice as much as that for silicon, which is expected to result in a groove profile reduction factor of approximately  $R = 2$ . Moreover, AR3 exhibits a very smooth surface and no significant roughness built-up during the plasma etch. The low surface roughness of the sacrificial layer is important since it is expected to be transferred to the Si facets with the ratio of  $V_{Si}/V_{SL}$ . This makes an AR3 coating very promising as a material for a sacrificial layer for the blaze angle reduction process.

AR3 was applied to the surface of the Si grating by spin-coating at 1000 rpm and then baked at  $200^\circ\text{C}$ . The liquid film provides planarization of the saw-tooth surface due to capillary forces, while centrifugal forces and volume shrinkage of the sacrificial layer during spin-coating and the baking reduce the planarization effect [14]. To achieve a high degree of planarization, the coating should be relatively thick. We applied 15 layers of the AR3 of total thickness of  $1.4 \mu\text{m}$  to planarize the micron deep grooves of the Si grating [Fig. 3(a)]. Residual waviness of the top surface of the AR3 coating did not exceed 7 nm peak-to-valley [Fig. 2(b)].

Reactive plasma etching using  $\text{CF}_4$  gas was applied to the planarized grating. The SEM image in Fig. 3(b) shows the grating in the middle of the reduction process when the grating grooves are half etched (corresponding to the stage shown in Fig. 1(c)). The bottom part of the grooves is still coated by the AR3 while the upper part of the grooves exposed to the  $\text{CF}_4$  plasma has a reduced slope of the facets.

AFM measurements of the fully processed grating showed that the blaze angle has been reduced approximately by a factor of 2, as expected [Fig. 4]. The reduction procedure was repeated 4 more times to achieve further reduction of the blaze angle. The change of the groove profile with successive reduction cycles is shown in Fig. 4. The final grating shown in Fig. 5 has the blaze angle of  $0.17^\circ$ , an almost perfect groove profile, plane and smooth facets with residual surface roughness of 0.6 nm rms.

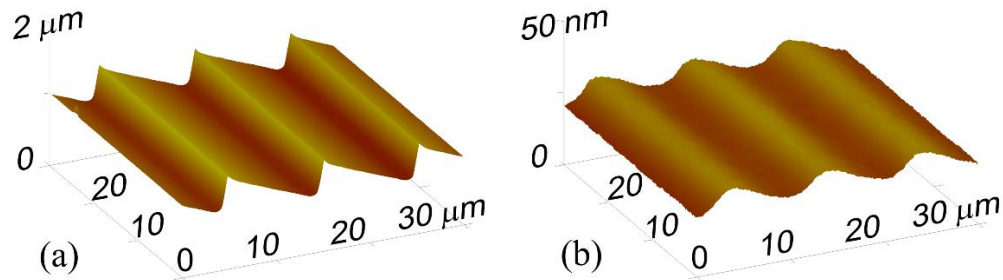


Fig. 2. AFM image of the blazed gratings with blaze angles of  $5.7^\circ$  before (a) and after (b) planarization. The full vertical range is  $2 \mu\text{m}$  and 50 nm respectively.

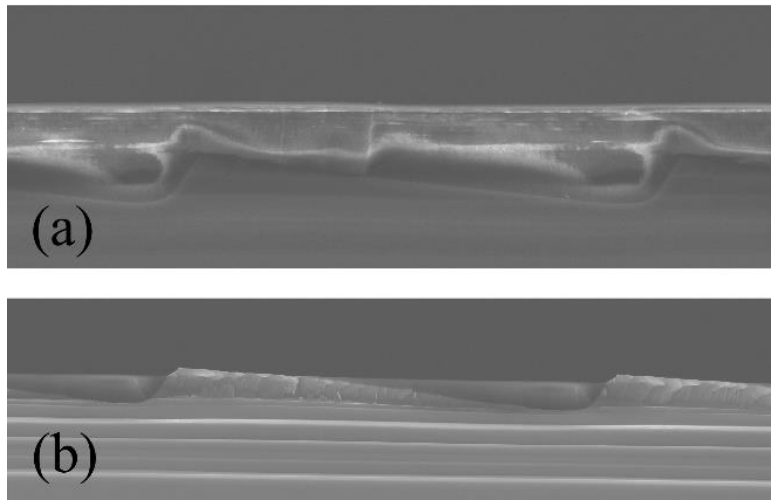


Fig. 3. Cross-sectional SEM images of an original 100 lines/mm grating with blaze angle of  $5.7^\circ$ , planarized with AR3 coating (a), (b) the same grating in the middle of the RIE reduction etch: the AR3 is still observed in the bottom part of the grooves, and the upper part of the grooves has a reduced blaze angle.

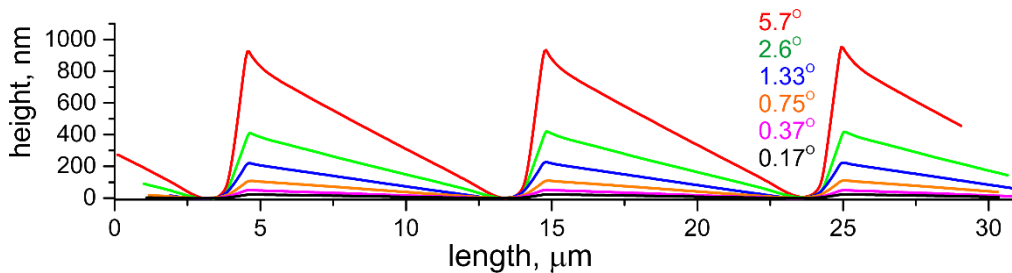


Fig. 4. Profiles of the grating before and after successive reduction cycles

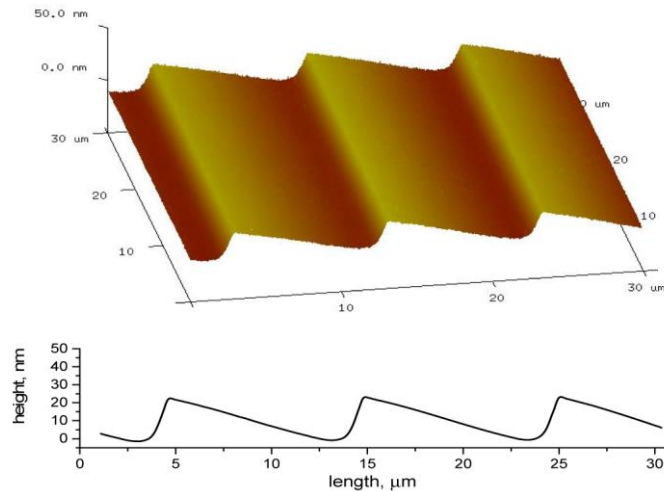


Fig. 5. AFM image and the average groove profile of the final blazed grating with a groove density of 100 lines/mm and a blaze angle of  $0.17^\circ$ .

#### 4. Diffraction efficiency

The low blaze angle grating was coated with an Au film and diffraction efficiency of the grating was measured over the soft x-ray energy range using the reflectometer at the beamline 6.3.2 of the Advanced Light Source [15]. Owing to small vertical beam size of 50  $\mu\text{m}$  a footprint of the beam on the grating did not exceed 5 mm for the whole energy range of 200 - 1300 eV, which was much smaller than the dimensions of the test grating. A diffraction pattern recorded by the detector scan at a constant incidence angle of  $88.46^\circ$  and an energy of 700 eV is shown by the blue curve in Fig. 6(a). Comparison to the similar diffraction data obtained for the Cosmic monochromator grating [Fig. 6(b)] clearly shows the advantage of the blazed grating over the lamellar one. Concentration of most of the diffraction energy into a single diffraction order by the blazed grating results in high diffraction efficiency, while the lamellar grating has at least two times lower efficiency due to almost even distribution of the diffracted energy between positive and negative orders.

The diffraction efficiency of the 1st positive order of the blazed grating measured over a wide energy range is shown in Fig. 7. The efficiency shown with the blue curve was measured for the grating set under the blazed condition, when the incident,  $\alpha$ , diffraction,  $\beta$ , and blazed,  $\phi$ , angles are related by  $(\alpha + \beta)/2 = \phi$ . The other set of measurements shown with the green curve were done at the constant grating focusing factor  $C_{\text{ff}} = \cos\beta/\cos\alpha = 1.2$ . Such a geometry is practically important for monochromator operation. Both measurements show almost the same efficiency up to the energy of 600 eV at which the blaze angle of  $0.17^\circ$  was optimized. For higher energies the constant  $C_{\text{ff}}$  geometry leads to some deviation from the perfect blaze condition, resulting in some reduction of the efficiency at the edges of the energy range. Nevertheless the efficiency of the blazed grating is approximately twice as high as compared to the efficiency of the lamellar Cosmic grating, shown with a red curve in Fig. 7. Additionally, the blazed grating offers high efficiency over a wider energy range as compared to the lamellar one, which gives a possibility to minimize the number of the gratings to cover a required energy range.

Simulations performed using PCGrate 6.1 software [16] show that diffraction efficiency of the fabricated blazed grating is very close to the theoretical efficiency calculated for an ideal saw-tooth groove profile (grey bars in Fig. 6(a)). The minor discrepancy between theoretical and experimental efficiency is caused by marginal imperfections of the groove profile of the fabricated grating, which is confirmed by efficiency simulations performed for the real groove profile measured with AFM (red bars in Fig. 6(a)).



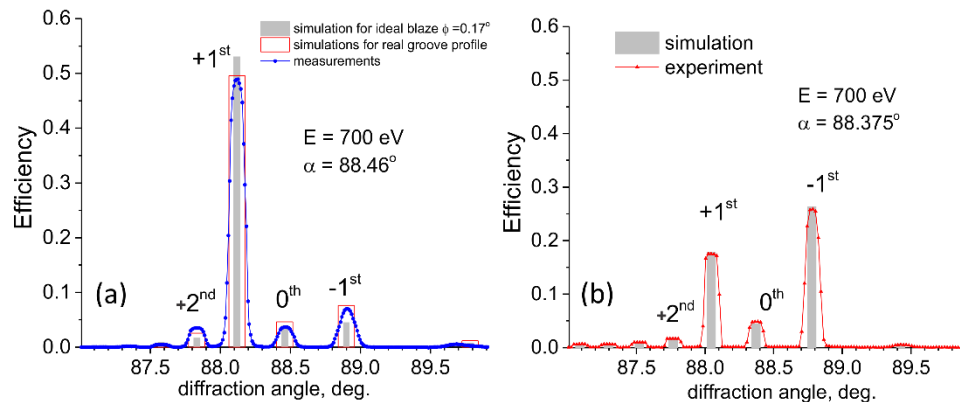


Fig. 6. Experimental (blue line with symbols) and simulated (red and grey bars) diffraction from the fabricated blazed grating at an energy of 700 eV and an incidence angle of  $88.46^\circ$  (a). Experimental (red line with symbols) and simulated (grey bars) diffraction efficiency of the 100 lines/mm lamellar grating from the Cosmic monochromator (b).

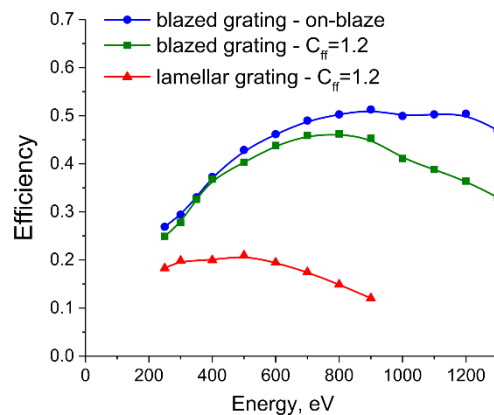


Fig. 7. Experimental efficiency of the 1st positive diffraction order of the 100 lines/mm Cosmic lamellar grating (red curve with triangular symbols) and the blazed grating under blaze conditions (blue curve with circle symbols) and for the constant  $C_{ff} = 1.2$  geometry (green curve with square symbols).

## 5. Summary

We developed a process of reduction of a blaze angle of Si blazed gratings which allows ultra-low blaze angle gratings required for synchrotrons and FELs. The method is based on planarization of the blazed grooves by a sacrificial layer and following plasma etching with a required etch ratio of the sacrificial layer and Si. This process provides very shallow grooves of a perfect saw-tooth profile and high diffraction efficiency of the modified blazed grating, close to the theoretical one. The reduction process can be applied for blazed gratings fabricated by any technique after certain recipe adjustments. The method opens the possibility to modify the blaze angle of existing gratings if necessary.

These experiments were conducted on a small test grating of size of 25 mm by 25 mm. For real x-ray applications a length of up to 200 mm is required. We have previously demonstrated fabrication of large area gratings using a nanoimprint technology [17,18] and this combined with the new method described here should yield large area low blaze angle gratings. Extrapolating from the current length of 25 mm to the required length of 200 mm will require careful attention to uniformity of the process but current results clearly demonstrate the feasibility of this approach. Further development of the approach would allow highly efficient gratings with blaze angles less than  $0.1^\circ$  for the 2 – 10 keV x-ray

energy range. This is a range covering the K absorption edges of Sulphur through the transition metals up to Zinc. This range is conventionally covered by Bragg crystals, such as Si (111). However the Bragg condition means that dispersion is only possible over the very narrow energy width of the Bragg reflection. So called dispersive crystal spectrometers have been developed for this range, but they are angle selecting rather than being truly dispersive, i.e. one angle on the crystal corresponds to one photon energy, and other energies are absorbed. This is not the case with a grating where due to the 2D nature of the diffraction rather than the 3D nature of Bragg reflection, all wavelengths less than the period can be dispersed. This type of medium energy grating-based dispersive spectroscopy should open a new realm in our ability to monitor chemical reactions in real time, via changes in the x-ray absorption spectrum.

### Disclaimer

This document was prepared as an account of work sponsored by the United States Government. While this document is believed to contain correct information, neither the United States Government nor any agency thereof, nor The Regents of the University of California, nor any of their employees, makes any warranty, express or implied, or assumes any legal responsibility for the accuracy, completeness, or usefulness of any information, apparatus, product, or process disclosed, or represents that its use would not infringe privately owned rights. Reference herein to any specific commercial product, process, or service by its trade name, trademark, manufacturer, or otherwise, does not necessarily constitute or imply its endorsement, recommendation, or favoring by the United States Government or any agency thereof, or The Regents of the University of California. The views and opinions of authors expressed herein do not necessarily state or reflect those of the United States Government or any agency thereof or The Regents of the University of California.

### Funding

Advanced Light Source and Molecular Foundry are supported by the Director, Office of Science, Office of Basic Energy Sciences, of the U.S. Department of Energy under Contract No. DE-AC02-05CH11231.

### References

1. J. Dvorak, I. Jarrige, V. Bisogni, S. Coburn, and W. Leonhardt, "Towards 10 meV resolution: The design of an ultrahigh resolution soft X-ray RIXS spectrometer," *Rev. Sci. Instrum.* **87**(11), 115109 (2016).
2. T. Warwick, Y.-D. Chuang, D. L. Voronov, and H. A. Padmore, "A Multiplexed High-Resolution Imaging Spectrometer for Resonant Inelastic Soft X-ray Scattering Spectroscopy," *J. Synchrotron Radiat.* **21**(Pt 4), 736–743 (2014).
3. D. Shapiro, S. Roy, R. Celestre, W. Chao, D. Doering, M. Howells, S. Kevan, D. Kilcoyne, J. Kirz, S. Marchesini, K. A. Seu, A. Schirotzek, J. Spence, T. Tyliczszak, T. Warwick, D. L. Voronov, and H. A. Padmore, "Development of coherent scattering and diffractive imaging and the COSMIC facility at the Advanced Light Source," *J. Phys. Conf. Ser.* **425**(19), 192011 (2013).
4. F. Siewert, B. Löchel, J. Buchheim, F. Eggenstein, A. Firsov, G. Gwalt, O. Kutz, S. Lemke, B. Nelles, I. Rudolph, F. Schäfers, T. Seliger, F. Senf, A. Sokolov, C. Waberski, J. Wolf, T. Zeschke, I. Zizak, R. Follath, T. Arnold, F. Frost, F. Pietag, and A. Erko, "Gratings for synchrotron and FEL beamlines: a project for the manufacture of ultra-precise gratings at Helmholtz Zentrum Berlin," *J. Synchrotron Radiat.* **25**(Pt 1), 91–99 (2018).
5. J. Gaudin, C. Ozkan, J. Chalupský, S. Bajt, T. Burian, L. Vyšín, N. Coppola, S. D. Farahani, H. N. Chapman, G. Galasso, V. Hájková, M. Harmand, L. Juha, M. Jurek, R. A. Loch, S. Möller, M. Nagasono, M. Störmer, H. Sinn, K. Saksı, R. Sobierajski, J. Schulz, P. Sovak, S. Toleikis, K. Tiedtke, T. Tschentscher, and J. Krzywinski, "Investigating the interaction of x-ray free electron laser radiation with grating structure," *Opt. Lett.* **37**(15), 3033–3035 (2012).
6. W. Jark and D. Eichert, "On symmetric X-ray beam splitting with high efficiency by use of reflection gratings with rectangular profile in the extreme off-plane configuration," *Opt. Express* **23**(17), 22753–22764 (2015).
7. W. Werner and H. Visser, "X-ray monochromator designs based on extreme off-plane grating mountings," *Appl. Opt.* **20**(3), 487–492 (1981).
8. K. F. Heidemann, B. Nelles, and R. Lenke, "Gratings with Blaze Angles Down to 0.1° for Photon Energies up to 10 keV," *AIP Conf. Proc.* **879**, 485–488 (2007).



9. D. Cocco, A. Bianco, B. Kaulich, F. Schaefer, M. Mertin, G. Reichardt, B. Nelles, and K. F. Heidemann, "From Soft to Hard X-ray with a Single Grating Monochromator," AIP Conf. Proc. **879**, 497–500 (2007).
10. D. L. Voronov, P. Lum, P. Naulleau, E. M. Gullikson, A. V. Fedorov, and H. A. Padmore, "X-ray diffraction gratings: precise control of ultra-low blaze angle via anisotropic wet etch," Appl. Phys. Lett. **109**(4), 043112 (2016).
11. D. L. Voronov, R. Cambie, E. M. Gullikson, V. V. Yashchuk, H. A. Padmore, Yu. P. Pershin, A. G. Ponomarenko, and V. V. Kondratenko, "Fabrication and characterization of a new high density Sc/Si multilayer sliced grating," Proc. SPIE **7077**, 707708 (2008).
12. D. L. Voronov, F. Salmassi, J. Meyer-Ilse, E. M. Gullikson, T. Warwick, and H. A. Padmore, "Refraction effects in soft x-ray Multilayer Blazed Gratings," Opt. Express **24**(11), 11334–11344 (2016).
13. <http://www.capitolscientific.com/Dow-Electronic-Materials-AR3-600-DUV-Anti-Reflectant-1-Gallon-Glass-Bottle>
14. L. E. Stillwagon and R. G. Larson, "Planarization during spin coating," Phys. Fluids A Fluid Dyn. **4**(5), 895–903 (1992).
15. <http://cxro.lbl.gov/reflectometer>
16. <http://www.pcgrate.com>
17. D. L. Voronov, E. M. Gullikson, and H. A. Padmore, "Large area nanoimprint enables ultra-precise x-ray diffraction gratings," Opt. Express **25**(19), 23334–23342 (2017).
18. D. L. Voronov, P. Lum, and H. A. Padmore, "Full size x-ray grating fabrication using large area nanoimprint," Proc. SPIE **10386**, 1038607 (2017).